Surface and Coating Technology, accepted, September 2004

The influence of the ion current density on plasma nitriding process

E. A. Ochoa, C. A. Figueroa, and F. Alvarez*

Instituto de Física "Gleb Wataghin", Universidade Estadual de Campinas – UNICAMP, C. P. 6165, 13083-970 Campinas, SP, Brasil

Elsevier use only: Received date here; revised date here; accepted date here.

Abstract

In this paper we report a comprehensive nitriding study carried out using low-alloy steel AISI 4140, combining nitrogen ion-beam-implantation and pulsed plasma nitriding. Quantitative relationships among hardness, nitrogen bulk profile concentration, and current ion densities are reported. The hardness profile showed a linear relationship with the nitrogen concentration. The samples were characterized by photoemission electron spectroscopy (XPS), X-rays diffraction analysis (XRD), scanning electron microscopy (SEM) and in-depth nano-hardness measurements. Samples treated by ion-beam-implantation showed the presence of a compound layer formed principally by e-Fe_3N and g'-Fe_4N. On the other hand, samples treated by pulsed plasma nitriding showed only the existence of g'-Fe_4N. In the later set of samples, was possible to prove that hardness is proportional to the ion current density.

Keywords: Nitriding; Hardness; Ionic Implantation.
PACS: 62.20.Q, 81.40.N, 52.75.R

1. Introduction

Plasma nitriding is an established method for surface hardening of metals, improving wear, friction, and corrosion resistance [1]. Nowadays, there are many plasma technologies in use but the correlation among ion current density, nitrogen profiles, and hardness is not well established. In spite of the few quantitative results reported there is a general consensus about the proportionality between hardness and nitrogen profiles [2,3]. This is probably due to the difficulties found in plasma pulsed plasma (PP) nitriding process to exactly measured the density of current and nitrogen concentration in the solid phase. Moreover, some questions related to the influence of the ion current density on the hardness and nitrogen concentration in-depth profile, remain unresolved. In contrast to PP nitriding, ion beam (IB) implantation using Kaufman cells presents excellent independent parameters control [4-6]. The fine adjustment of current, energy, and ion beam composition makes this technique unique for detailed nitriding studies. Therefore, experiments using IB can give an important contribution to the subject, and being aware of the peculiarities involved in each technique, these results can help to understand other phenomena as those found in PP. Taking advantage of these possibilities, several researchers recently reported important works studied using IB, considering different ion energy conditions, intensity, and implantation times [4,7-11].

In the present paper we report a comprehensive nitriding carried out employing AISI 4140 steel, combining nitrogen IB and PP as treatment techniques and photoemission electron spectroscopy (XPS), X-rays diffraction analysis (XRD), scanning

* *Corresponding author.* Tel.: +55-19-3788-5372 ; fax: +55-19-37885376;

E-mail address: alvarez@ifi.unicamp.br.

electron microscopy (SEM), and in depth nano-hardness measurements, as characterization tools. Quantitative relationships among hardness, nitrogen bulk profile concentration, and ion current densities are reported. Finally, a method to estimate nitrogen profile and current density from the hardness vs. depth curves is presented and applied to AISI 4140 steel samples treated in a pulsed plasma apparatus.

2. Experimental

Rectangular AISI 4140 samples, 10 x 20 mm and 1mm thick, from the same source were used for all the experiments (C%: 0,4; Si%: 0,25, Cr%: 1,0; Mo%: 0,20, Mn%: 0,85, P%: < 0,40, S%: < 0,40; Fe: balance). The samples were mirror polished using standard metallographic techniques. The nitriding experiments were performed in a PP system and an IB apparatus with a 3-cm diameter DC Kaufman ion source. More detailed descriptions of the implantation system are found elsewhere [12]. The implantation system containing the Kaufman cell is attached to an ultra high vacuum system for XPS measurements. The background chamber pressure is $< 10^{-4}$ Pa. The gases are introduced in the Kaufman ion source through mass flow-meter controllers and the ions impact normal to the surface of the samples. The chamber pressure is monitored using a Varian cold cathode gauge. The absolute pressure values are obtained using the appropriate gas correction factor provided by the manufacture. The samples studied by pulsed plasma nitriding were obtained at 520 ^{o}C while those obtained by IB process at 550 °C. The nominal nitrogen current density of the ion beam was fixed in all experiments. The nominal current is obtained by dividing the beam current of the Kaufman ion source by the geometrical beam area. This current density must be interpreted as the initial one leaving the gun. However, depending on the total pressure in the chamber, i.e., the scattering introduced by background molecules, different current densities are measured at the surface sample. A Faraday cup was used to know the true current densities arriving at the sample [13,4]. Completing the main experimental conditions, the nominal ion energy of the beam was fixed at 600 eV.

The plasma apparatus consists of a hot wall furnace with 200 Kg load capacity powered by a pulsed source of 1000 V and 60 A maximum voltage and current, respectively. The pulse width can be varied from 20 to 1500 μs in 1μs steps and the current is stabilized within 0.1 % in current. The 80 cm high and 50 cm useful load zone is controlled within 3 °C, spatially and temporally. The samples were deposited using a 200 μs length pulse, 50 μs duty and 430 V. In this case the temperature of the samples was of 520°C.

Table 1. Deposition parameters used in the experiments. PP and IB stand for pulsed plasma and ion beam deposited samples, respectively.

Sample	Time (hours)	T (^{0}C)	Density (mA/cm^2)	Current (A)	[N]/[N+H] %
IB1	1	550	1.20	40	100
IB2	4	550	1.20	40	100
IB3	9	550	1.20	40	100
PP1	15	520	1.55	10	67
PP2	15	520	1.50	9.5	67
PP3	15	520	1.26	6.3	67
PP4	15	520	1.24	5.0	67
PP5	15	520	1.11	3.5	67

The deposition conditions are displayed in Table 1. PPx identifies samples deposited in the pulsed plasma system while those implanted with the Kaufman cell by IBx. Here, x stands for the identification sample number.

The hardness measurements were performed in two ways. The hardness of the IB samples were measured perpendicular to the nitrided surface following the procedure explained below. The hardness of samples nitrided by pulsed plasma were measured on cross-section, i.e., the samples were sliced perpendicularly to the nitrided surface and mirror polished before indenting measurements. In all the nitrided samples, the hardness was obtained using a Berkovich diamond tip (NanoTest-300) and the results analysed using the Oliver and Pharr method [14]. Piling-up effects were not considered. The indentation initial load was the ~ 0.1 mN and the indentation velocity of ~ 3.45 mN.s^{-1}. Each reported hardness measurement was obtained averaging five indentation curves. The average standard deviation was around 5 %. The cross-section morphology and the thickness of the nitrided layers were measured from SEM images (JEOL JMS-5900LV). The nitrided layers were revealed, at room temperature, by etching the samples with Marble's solution. The X-ray patterns were obtained with the Cu Kα (l = 1,54 Å) line, 40 kV and 30 mA current.

The in-depth profile of the N concentration of the IB samples was performed as follows. After implantation, the IB samples were transferred to the XPS chamber for compositional analysis. The ***in situ*** profiling of the nitrogen concentration was obtained by sputtering the sample in the IB chamber by a 1KeV Ar^+ beam coming out from the Kaufman cell.

In this condition, a 0.2 μm/min erosion rate was obtained. This process was repeated several times until 50 μm depth was reached. Above this thickness, the erosion was performed by *ex situ* 100 μm steps mechanical wearing. The sample was then reintroduced in the IB chamber and a 3 minutes Ar^+ sputtering clean up procedure was applied. Therefore, the sample was again transferred into the XPS chamber for N concentration measurements. This procedure is repeated several times until a depth of ~ 1mm was reached.

3. Results and discussion

3.1 X-rays diffraction results

Figure 1 (a) shows the diffraction patterns for the samples IB1, IB2 and IB3 immediately after implantation. For comparison purposes, the diffraction pattern of an untreated sample is also displayed. In this pattern, the structure associated with the original a-Fe phase is present. Also, the presence of the e-$Fe_{2,3}N$ (7.7 – 9.5 wt% N) and g´-Fe_4N (~ 6 wt% N) phases are also present [15]. Moreover, it is clearly seen an increment in the proportion of the e-$Fe_{2,3}N$ phase at higher implantation times. Fig. 1 (b) shows a (selected) sequence of diffraction patterns corresponding to the IB3 sample. The patterns were obtained after successive mechanical erosion, of the samples surface. As it is observed in the graph, the g´ phase is still present after the e phase had disappeared. Moreover, above ~100 μm depth no different phases other that a-Fe are observed, indicating that the *diffusion* region of the case was reached. In next section, we shall see that this phase extended up to ~800 μm depth. Following the sequence (partially showed in Fig. 1(b)), one can conclude that the compound formed by implantation (~20 μm thick layer) is constituted by two single phases, i.e., e and g´. Indeed, this is confirmed by the direct measurements from the SEM images. It is interesting to remark that the nitrogen concentration at 100 μm in depth is ~ 2.2 wt % (see below in Fig. 3) exceeding the limit of 0.1 wt % for nitrogen saturation in a-Fe (ferrite) pure. Indeed, Muñoz-Páez et al. [16] have proved that the presence of elements such as chromium, vanadium, and others transition metals, can stabilize a super-saturate a-bcc phase of iron avoiding the transformation to g´.

Figure 2 shows the X-rays diffraction pattern of the samples treated by pulsed plasma (PP1, PP3, and PP5) at different effective total currents delivered into the furnace (see table 1). As observed in these diffraction patterns, only the g´-Fe_4N phase is present. For the sample deposited at the smallest current, an ill-defined peak associated to a-Fe is visible, indicating that there is a substantial difference when compared to the corresponding patterns observed for the IB process (i.e., total absence of the e-$Fe_{2,3}N$ phase). This is probably due to the nitriding parameters used in the process.

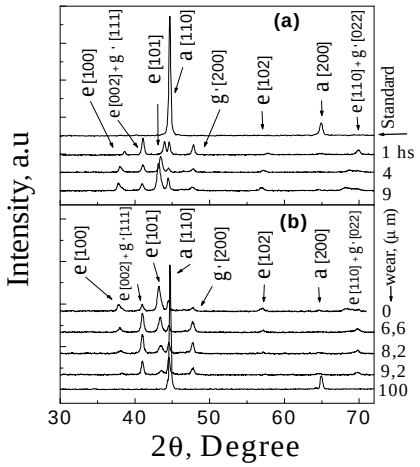

Figure 1. a) Diffraction patterns of as received (standard) and nitrided samples at different treatment times (see Table I). b) Examples of X-rays pattern for the IB3 sample at different depths. The wear thicknesses are indicated. The curves are arbitrarily shifted.

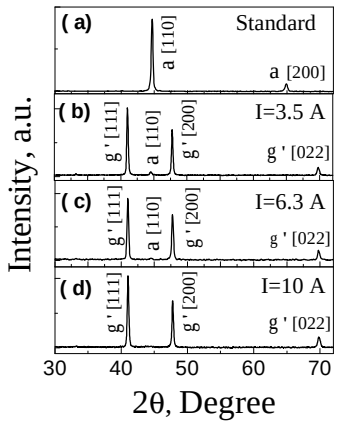

Figure 2. Diffraction patterns of the AISI 4140 samples treated by pulsed plasma. Only the γ´ phase is observed.

3.2 Concentration and hardness profiles: structural correlation I

The nitrogen concentration and the hardness of the sample IB3 were determined after the successive erosion procedure, as explained in section 2. Figure 3 the shows nitrogen concentration and the hardness as a function of the sample depth

They were arbitrarily scaled in such a way to put in evidence the correlation between these two physical quantities. This correlation is more apparent in Figure 4, where we have plotted hardness versus nitrogen at each corresponding depth for concentration greater than 2 wt%, i.e., smaller depth than ~100 μm. At very shallow depth, the measure of nitrogen concentration contains a considerable experimental error. So, it was not considered. Therefore, above 2 % wt. of nitrogen concentration, the remarkable linearity confirms the proportionality between nitrogen and hardness.

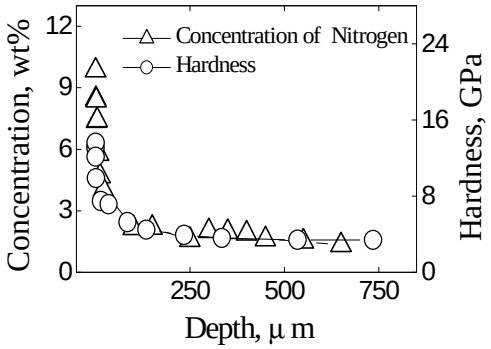

Figure 3. Concentration and hardness curves vs depth for the sample IB3.

The proportionality observed has important practical consequences. Indeed, the hardness curves are easier to obtain than the nitrogen concentration profiles. Therefore, assuming that the proportionality factor is experimentally determined, the hardness curves could be transformed in nitrogen concentration profiles. This is true, independently of the nitriding technique used, *provided that similar phases are present in the material*. This assumption presumes that, for equals material composition and previous heat treatment, the material hardness will only depend on nitrogen concentration. Therefore, one can applied this approach to estimate the effective nitrogen concentration and the ion current density employed during the process. Moreover, as the current is well known in the IB experiments (1.2 mA/ cm^2), the efficiency of nitrogen incorporation can be estimated.

We call attention, finally, that the proportionality between hardness and nitrogen concentration displayed in Figure 4 was determined in the region where the e-$Fe_{2,3}N$, g´-Fe_4N, and a-Fe phases were present.

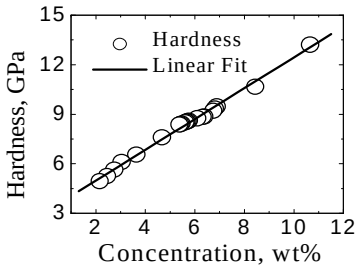

Figure 4. Hardness vs nitrogen concentration curve displaying the proportionality between these quantities.

3.3 Current density and hardness: structural correlation II

Figure 5 (a) shows the effective current density vs. nominal current. Figure 5 (b) shows the hardness vs. depth of the samples obtained by pulsed plasma nitriding. According to the arguments discussed above, the hardness is proportional to nitrogen concentration, i.e., $\mathbf{H(x) = k\,A\,N(x).}$ Here k is a constant, $\boldsymbol{A}$ is the sample area, $\mathbf{N(x)}$ is the nitrogen concentration, and $\mathbf{x}$ indicates the co-ordinates perpendicular to sample surface. Therefore, the total number of nitrogen implanted atoms is $\mathbf{n = (k\,A)^{-1}} \int_0^{\infty} \mathbf{H(x)} = \mathbf{(k\,A)^{-1}\,A_{PP}}$, where $\mathbf{A_{PP}} = \int_0^{\infty} \mathbf{H(x)}$ represents the area below the hardness curves (Figure 5(b)). Furthermore, assuming $\mathbf{n}$ proportional to the total particles landing on the sample during the deposition time $\mathbf{T_{PP}}$, due to the ion density of current $\mathbf{J_{PP}}$, we have:

$$\mathbf{n = (k\,A)^{-1}\,A_{PP} = J_{PP}\,T_{PP}\,A}, \qquad [1]$$

Combining this expression with similar one for the sample IB3, we have:

$$\mathbf{J_{PP} = J_{IB}\,(A_{PP}/\,T_{PP})\,/\,(A_{IB}/\,T_{IB})} \qquad [2]$$

Here, $\mathbf{J_{IB}}$, $\mathbf{A_{IB}}$, $\mathbf{T_{IB}}$, are the current density, the area below the hardness curve, and deposition time, respectively for the ion beam implanted sample IB3.

To arrive to this relationship we have assumed the same ***k*** constant and the same sample areas.

In conclusion, equation [2] gives the effective current density $\mathbf{J_{PP}}$ of the pulsed plasma process assuming the total areas below the hardness curves, the deposition times, and the density of current in the ion source implanted samples are known. Using the expression [2] and the measured $\mathbf{J_{IB}}$ = 1.2 mA/cm^2 for sample IB3, the effective currents during the pulsed plasma treatment were obtained (Figure 5, a).

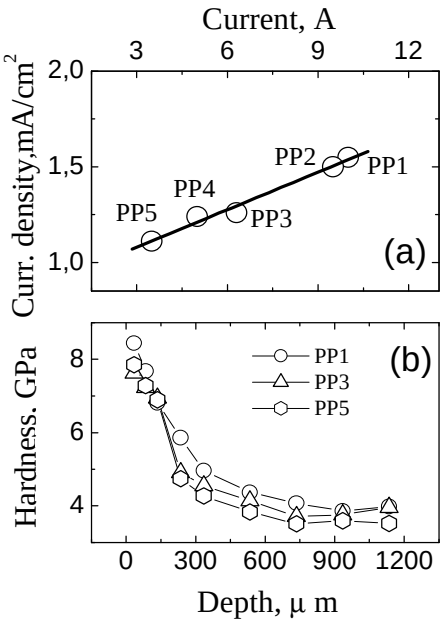

Figure 5. (a) Left axis: effective current density during plasma pulsed nitriding using the correlation obtained from figure 3 as a function of depth. Top axis: nominal current in the plasma pulse experiments; (b) Hardness vs. depth during the pulsed plasma nitriding. For the sake of clarity, only a selected group of curves are displayed in this panel.

Finally, Figure 6 shows the hardness vs. plasma current at two different depths corresponding to the samples treated by the pulsed plasma process. The curves, obtained from Figure 5, show a linear correlation between the hardness and the plasma current.

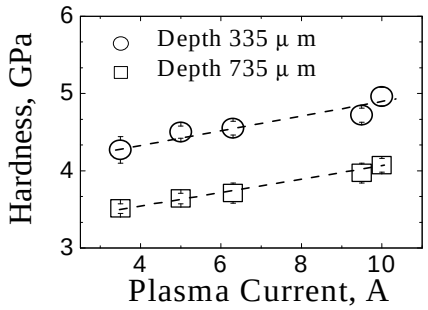

Figure 6. Hardness vs plasma current, for ~ 335 μm and 735 μm depth corresponding to the plasma pulsed samples.

4. Conclusions

Samples of low-alloy steel AISI 4140 were nitrided by ion beam implantation and pulsed plasma process. A linear correlation between the hardness and the nitrogen profile was established for nitriding samples implanted using an ion source, i.e., the hardness in-depth curves mapped the nitrogen profile concentration.

A method to estimate nitrogen profile and current density for AISI 4140 steel nitrided by pulsed plasma was presented. The method uses the hardness vs. depth curves and the following assumptions are involved. Firstly, the nitrogen profile of a the sample must be known, the ion current density used in its preparation, and the phases present in the material. Second, the crystalline phases of the unknown nitrided material must be similar to the well-characterized sample. Finally, the hardness vs. depth curves must be known. Under these assumptions, the area under the hardness curves is proportional to nitrogen concentration.

Acknowledgments

This work is part of the Master degree requirements of EAO. The authors are grateful to D. Ugarte and M. Bica for their help with some measurements. Thanks to D. Wisnivesky for helping in the preparation of some samples and interesting discussions. The work was partially sponsored by FAPESP. CAF and EAO are FAPESP fellows. FA is CNPq fellow.

References

[1] A.H. Deutchman, R. J. Partyka, C. Lewis, Conference Proceedings of the ASM - 2nd Int. Conf., Cincinati, Ohio, USA, p. 29 (1989). Edited: by T. Spalvins and W. L. Kovacs, ASM Int., Mat. Park, Ohio 44073, USA.

[2] L. H. Corredor, B. Chornik, K. Ishizaki, Scripta Metallurgica 15 (1981) 195.

[3] I. Alphonsa, A. Chainami, P. M. Raole, B. Ganguli, P. I. John, Surf. Coat. Tech. 146-150 (2002) 263.

[4] C. A. Figueroa, E. Ochoa, F. Alvarez, J. Appl. Phys. 94 (2003) 2242.

[5] C. A. Figueroa, D. Wisnivesky, P. Hammer, R. G. Lacerda, R. Droppa Jr., F. C. Marques, F. Alvarez, Surf. Coat. Tech. 146-147 (2001) 405.

[6] H.R. Kaufman, J. Vac. Sci. Technol**.** 15 (1978) 272.

[7] R. Wei, Surf. Coat. Technol. 83 (1996) 216.

[8] R. Wei, J. J. Vajo, J. N. Matossian, P. J. Wilbur, J. A. Davis, D. L. Williamson G. A. Collins, Surf. Coat. Technol. 83 (1996) 235.

[9] S. Leigh, M. Samandi, G. A. Collins, K. T. Short, P. Martin, L. Wielunsky, Surf. Coat. Technol. 85 (1996) 37.

[10] P. J. Wilbur, J. A. Davis, R. Wei, J. J. Vajo, D. L. Williamson, Surf. Coat. Technol. 83 (1996) 250.

[11] S. J. Bull, A. M. Jones, A. R. McCabe, Surf. Coat. Technol. 83 (1996) 257.

[12] P. Hammer, N. M. Victoria, F. Alvarez, J. Vac. Sci. Technol. A 16 (1998) 2491.

[13] H. Ch. Paulini, U. Littmark, Nuc. Inst. Meth. Phys. Res. B 58 (1991) 260.

[14] W. C. Oliver, G. M. Pharr, J. Mater. Res. 7 (1992) 1564.

[15] L.Torchane, P. Bilger, J. Dulcy, and M. Gantois, Metall. Mater. Trans. A, 27A (1996) 1823

[16] A. Muñoz-Páez, J. I. F. Peruchena, J. P. Espinós, A. Justo, F. Castañeda, S. Días-Moreno, D. T. Bowron, Chem. Mater. 14 (2002) 3220.